Generation and Distribution of a Wide-Band Continuously Tunable Millimeter-Wave Signal With an Optical External Modulation Technique

Guohua Qi, Jianping Yao, *Senior Member, IEEE*, Joe Seregelyi, Stéphane Paquet, and Claude Bélisle

***Abstract*—A new technique to generate and distribute a wide-band continuously tunable millimeter-wave signal using an optical external modulator and a wavelength-fixed optical notch filter is proposed. The optical intensity modulator is biased to suppress the odd-order optical sidebands. The wavelength-fixed optical notch filter is then used to filter out the optical carrier. Two second-order optical sidebands are obtained at the output of the notch filter. A millimeter-wave signal that has four times the frequency of the microwave drive signal is generated by beating the two second-order optical sidebands at a photodetector. Since no tunable optical filter is used, the system is easy to implement. A system using an $LiNbO_3$ intensity modulator and a fiber Bragg grating filter is built. A stable and high spectral purity millimeter-wave signal tunable from 32 to 50 GHz is obtained by tuning the microwave drive signal from 8 to 12.5 GHz. The integrity of the generated millimeter-wave signal is maintained after transmission over a 25-km standard single-mode fiber. Theoretical analysis on the harmonic suppression with different modulation depths and filter attenuations is also discussed.**

***Index Terms*—Electrooptic modulator, fiber Bragg grating (FBG), microwave photonics, millimeter-wave generation, optical heterodye.**

I. Introduction

GENERATION and transmission of microwave and millimeter-wave signals over optical fibers are of great interest for applications such as broad-band wireless access networks operating at millimeter-wave bands, antenna remoting, phased-array antennas, optical sensors, and radars [1]–[5]. Optical generation and transmission of electrical signals have been extensively investigated with most work to date focused on high-frequency signals, especially millimeter-wave signals. This is because there are fewer difficulties with conventional electronic techniques or optical techniques in generating and distributing lower-frequency electrical signals. Furthermore, the low-frequency modulated double-sideband (DSB) optical signal suffers less from the chromatic dispersion of the fiber than that of the high-frequency modulated signal when transmitting over standard single-mode fiber (SSMF) [6]–[8].

Manuscript received January 18, 2005. The work was supported by the Canadian Institute for Photonic Innovations.

G. Qi and J. Yao are with the Microwave Photonics Research Laboratory, School of Information Technology and Engineering, University of Ottawa, Ottawa, ON, Canada K1N 6N5 (e-mail: jpyao@site.uottawa.ca).

J. Seregelyi, S. Paquet, and C. Bélisle are with the Communications Research Centre, Ottawa, ON, Canada K2H 8S2.

Digital Object Identifier 10.1109/TMTT.2005.855123

Therefore, the highest frequency of the signal produced by these DSB techniques is limited by the bandwidth of the laser or the external modulator and the fiber chromatic dispersion. To overcome these limitations, an optical generation scheme that uses narrow bandwidth optical components to generate high-frequency electrical signals becomes attractive.

Optical microwave or millimeter-wave signal generation is usually based on heterodyne techniques by beating two optical carriers separated by the desired frequency in a square-law photodetector (PD). If the offset frequency of the two optical carriers is stable and their phases are correlated, a high-quality electrical signal will be generated. However, after the transmission of the two optical carriers over an SSMF, the generated microwave or millimeter-wave signal quality will be deteriorated because of the fiber chromatic dispersion [9].

Electrical signal generation based on optical heterodyning can be achieved by using either two stabilized lasers or one laser with an external optical modulator. The quality of the electrical signal produced by beating two free-running lasers rarely meets application specifications. Methods to further improve the signal quality, such as optical injection locking [10], [11] and optical phase-locked loop (OPLL) [12], [13], have been proposed. The OPLL techniques allow the suppression of the low-frequency components of the phase noise that deteriorate the generated signal. However, it is difficult to suppress the high-frequency components of the phase noise unless very narrow linewidth (in kilohertz) optical sources are used [14].

Methods using a laser with an external optical modulator, such as an optical intensity modulator or optical phase modulator, have shown great potential for producing high-purity high-frequency millimeter-wave signals. These approaches are based on the inherent nonlinearity of the response of the optical modulator for generating high-order optical sidebands. Taking advantage of this property can dramatically lower the bandwidth requirements for the optical modulator and allows the use of a much lower frequency electrical drive signal. This can greatly reduce the cost of the system and makes it more practical to use.

A method to generate millimeter-wave signals using an external optical modulation technique was proposed by O'Reilly *et al.* in 1992 [15]. A frequency-doubled electrical signal was optically generated by biasing the Mach–Zehnder modulator (MZM) to suppress even-order optical sidebands. A 36-GHz millimeter-wave signal was generated when the MZM was driven by an 18-GHz microwave signal. Such a system was employed for a remote delivery of video services [16].

In 1994, O'Reilly and Lane [17] proposed another method to generate a frequency-quadrupled electrical signal. Instead of biasing the MZM to suppress the even-order optical sidebands, the method [17] was based on the quadratic response of an optical intensity modulator. The optical carrier and the first- and third-order optical sidebands were suppressed by adjusting the drive signal level. A 60-GHz millimeter-wave signal was generated when a 15-GHz drive signal was applied to the MZM. However, to ensure a clean spectrum at the output of a PD, an imbalanced Mach–Zehnder filter with a free spectral range (FSR) equal to the spacing of the two second-order optical sidebands are used to suppress the unwanted optical components. Recently, an approach using an optical phase modulator to generate a frequency-quadrupled electrical signal was proposed [18]. In this approach, a Fabry–Perot filter was used to select the two second-order optical sidebands. An electrical signal that has four times the frequency of the electrical drive signal was generated by beating the two second-order sidebands at a PD. A key advantage of these approaches [17], [18] is that an optical modulator with a maximum operating frequency of 15 GHz can generate an millimeter-wave signal up to 60 GHz. However, since both approaches rely on the optical filter to select the two optical sidebands to generate tunable millimeter-wave signals, a tunable optical filter must be used, which significantly increases the complexity and the cost of the system.

For system applications with frequency reconfigurability, such as a wide-band surveillance radar, spread-spectrum or software-defined radio (SDR), continuously tunable millimeter-wave signals are highly desired. The prospect of generating a wide-band continuously tunable single-frequency millimeter-wave signal using fixed optical filters and narrow bandwidth optical modulators becomes very attractive. In this paper, we propose a new approach that can optically generate a wide-band continuously tunable millimeter-wave signal without using a tunable optical filter. The system employs an optical intensity modulator, which is biased to suppress the odd-order optical sidebands. A fiber Bragg grating (FBG) serving as a wavelength fixed notch filter is then used to filter out the optical carrier. A stable low-phase noise millimeter-wave signal at four times the frequency of the electrical drive signal is generated at the output of a PD. A 32–50-GHz millimeter-wave signal is observed on an electrical spectrum analyzer (ESA) when the electrical drive signal is tuned from 8 to 12.5 GHz. The quality of the generated millimeter-wave signal is maintained after transmission over a 25-km SSMF.

II. Analysis

A. Principle of the Proposed Approach

The proposed millimeter-wave signal generation system is shown in Fig. 1. An electrical drive signal is applied to an MZM. The MZM is biased to suppress the odd-order optical sidebands. An optical notch filter is connected at the output of the MZM to remove the optical carrier. Two second-order optical sidebands are obtained at the output of the notch filter. A beat signal with four times the frequency of the electrical drive signal is generated at a PD.

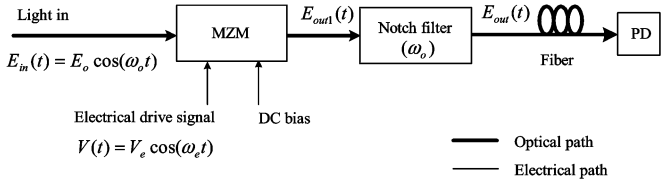

Fig. 1. Diagram of the proposed microwave signal generation system.

It is known that the electric field at the output of a lithium–niobate MZM, i.e., $E_{\text{out1}}(t)$, can be approximately expressed by

$$E_{\text{out1}}(t) = E_o \cos\left[\frac{\Phi\big[V(t)\big]}{2}\right] \cdot \cos(\omega_o t) \tag{1}$$

where E_o and ω_o are, respectively, the electric field amplitude and angular frequency of the input optical carrier, $V(t)$ is the applied electrical drive voltage, and $\Phi\big[V(t)\big]$ is the optical phase difference caused by $V(t)$ between the two arms of the MZM. If the MZM is driven by a sinusoidal electrical signal and biased with a constant dc voltage, $\Phi\big[V(t)\big]$ is expressed as

$$\Phi\big[V(t)\big] = \phi_0 + \frac{\pi}{V_\pi} \cdot V_e \cos(\omega_e t) \tag{2}$$

where ϕ_0 is a constant phase shift determined by the constant dc-bias voltage, V_π is the half-wave voltage at high frequency, and V_e and ω_e are the amplitude and angular frequency of the electrical drive signal, respectively. Substituting (2) into (1), the electric field of the output optical signal can be written as

$$\begin{aligned} E_{\text{out1}}(t) &= E_o \cos\left(\frac{\phi_0}{2}\right) J_0(\beta)\cos(\omega_o t) + E_o \cos\left(\frac{\phi_0}{2}\right) \\ &\quad \times \left\{\sum_{n=1}^{\infty} J_{2n}(\beta)\big[\cos(\omega_o t - 2n\omega_e t + n\pi) \right. \\ &\qquad \left. + \cos(\omega_o t + 2n\omega_e t - n\pi)\big]\right\} \\ &\quad - E_o \sin\left(\frac{\phi_0}{2}\right) \\ &\quad \times \left\{\sum_{n=1}^{\infty} J_{2n-1}(\beta)\left[\sin\left(\omega_o t - (2n-1)\omega_e t + n\pi - \frac{\pi}{2}\right)\right.\right. \\ &\qquad \left.\left. - \sin\left(\omega_o t + (2n-1)\omega_e t - n\pi + \frac{\pi}{2}\right)\right]\right\} \end{aligned} \tag{3}$$

where J_n is the Bessel function of the first kind of order n and $\beta = (V_e/V_\pi)\cdot(\pi/2)$ is the phase modulation index.

When the MZM is driven by an electrical signal with adequate power, a large value of β is obtained. In this case, (3) shows that the power in the input optical carrier will be spread out among the first-order, second-order, third-order, and higher order optical sidebands. The amplitude distribution of these sidebands is governed by the variation of Bessel functions parameterized by β. Their amplitude is also affected by ϕ_0. If all these optical

sidebands are fed to a square-law PD, harmonics of the electrical drive signal will be generated. The parameters β and ϕ_0 can be optimized, from the point-of-view of obtaining higher order electrical harmonics and maximizing its conversion efficiency. For example, ϕ_0 is tuned to suppress all even-order optical sidebands so that the power of all even-order sidebands is transferred to the odd-order ones [15]. An efficiency-improved frequency-doubled electrical signal is then obtained.

In our proposed method, the dc bias of the MZM is tuned to have $\phi_0 = 0, 2\pi, 4\pi, \ldots$. All the odd-order optical sidebands associated with the term $\sin(\phi_0/2)$ then vanish, as indicated in (3). Only the even-order optical sidebands are kept. The power in the odd-order optical sidebands is transferred to the even-order sidebands, improving the signal generation efficiency. If the electrical drive signal is applied to the MZM with an appropriate power level, optical sidebands up to the second order are generated and all optical sidebands above the second order have an amplitude low enough to be ignored, but the optical carrier, represented by the term with the zeroth-order Bessel function (J_0) in (3), is still part of the spectrum. The optical signal can then be approximately expressed as

$$E_{\text{out1}}(t) \cong E_o J_0(\beta)\cos(\omega_o t) - E_o J_2(\beta)\cos(\omega_o t - 2\omega_e t) - E_o J_2(\beta)\cos(\omega_o t + 2\omega_e t). \quad (4)$$

When this optical signal is fed to a PD, a strong frequency-doubled electrical signal and a weaker frequency-quadrupled electrical signal will be generated. However, when this optical signal that is composed of two second-order sidebands and one optical carrier is transmitted over a long span of optical fiber, the frequency-doubled electrical signal suffers from the chromatic-dispersion-induced power penalty [6]–[8], which limits its applications. In addition, the presence of a frequency-doubled electrical signal will cause interference to the operation of the frequency-quadrupled electrical signal in a wide-band system application. To eliminate the frequency-doubled electrical signal, we propose the use of a wavelength-fixed optical notch filter to filter out the optical carrier, as shown in Fig. 1. The electric field of the optical signal at the output of the optical notch filter can then be approximately expressed as

$$E_{\text{out}}(t) \cong -E_o J_2(\beta)\big[\cos(\omega_o t - 2\omega_e t) + \cos(\omega_o t + 2\omega_e t)\big]. \quad (5)$$

Therefore, at the output of the optical notch filter, only two optical sidebands separated by four times the frequency of the drive signal are present. Applying this optical signal to a PD, an electrical signal that has four times the frequency of the electrical drive signal will be generated. The generated electrical signal V_{out} can be written as

$$V_{\text{out}}(t) = C J_2^2(\beta)\cos(4\omega_e t) \quad (6)$$

where C is a constant that is related to the responsivity of the PD. Since the two optical sidebands originate from the same optical source, the frequency stability and phase noise of the generated signal are predominately determined by the electrical drive signal. Equation (6) also shows that the amplitude of the generated electrical signal can be maximized by optimizing the value $J_2(\beta)$.

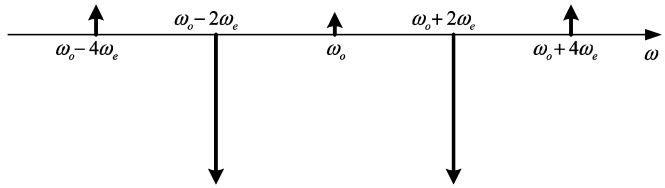

Fig. 2. Illustration of the optical spectrum at the output of the optical notch filter.

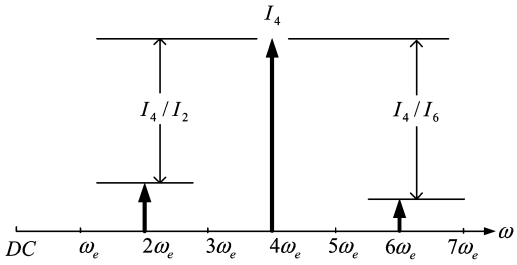

Fig. 3. Illustration of the electrical spectrum at the output of a PD.

It is important to note that the dc-bias level for which the odd-order optical sidebands are eliminated is not dependent on the frequency of the electrical drive signal. In addition, the optical carrier has a fixed wavelength; therefore, the optical notch filter does not need to be tunable. These characteristics ensure that the proposed approach can generate a frequency-tunable electrical signal by simply tuning the frequency of the electrical drive signal at a low-frequency band.

B. Electrical Harmonic Suppression Analysis

Usually in a wide-band electrical heterodyne system, especially when the system operates over an octave bandwidth, an electrically tuned bandpass filter is inserted between the local oscillator and the mixer to suppress unwanted harmonics. This prevents potential in-band interference from corrupting the receive signal. However, the use of an electrically tunable filter makes the system very complicated. A direct solution to this problem is to use a highly harmonic-suppressed local oscillator. In the following, we will analyze the harmonic-suppression characteristics of the proposed approach.

Assume that all odd-order optical sidebands generated by the modulation of the MZM by a sinusoidal signal can be completely suppressed by using an appropriate dc-bias voltage. That means that the condition of $\phi_0 = 0, 2\pi, 4\pi, \ldots$, is satisfied with a constant dc bias. Assume also that the attenuation of the optical notch filter at its center notch wavelength is in α dB. Based on the above assumptions, from (3), the optical signal at the output of the optical notch filter can be written as

$$E_{\text{out}}(t) = E_o k J_0(\beta)\cos(\omega_o t) + E_o \times \left\{ \sum_{n=1}^{\infty} J_{2n}(\beta)\big[\cos(\omega_o t - 2n\omega_e t + n\pi) + \cos(\omega_o t + 2n\omega_e t - n\pi)\big] \right\} \quad (7)$$

where k is the optical electrical field attenuation factor, which is related to α by $\alpha = -20\log_{10} k$.

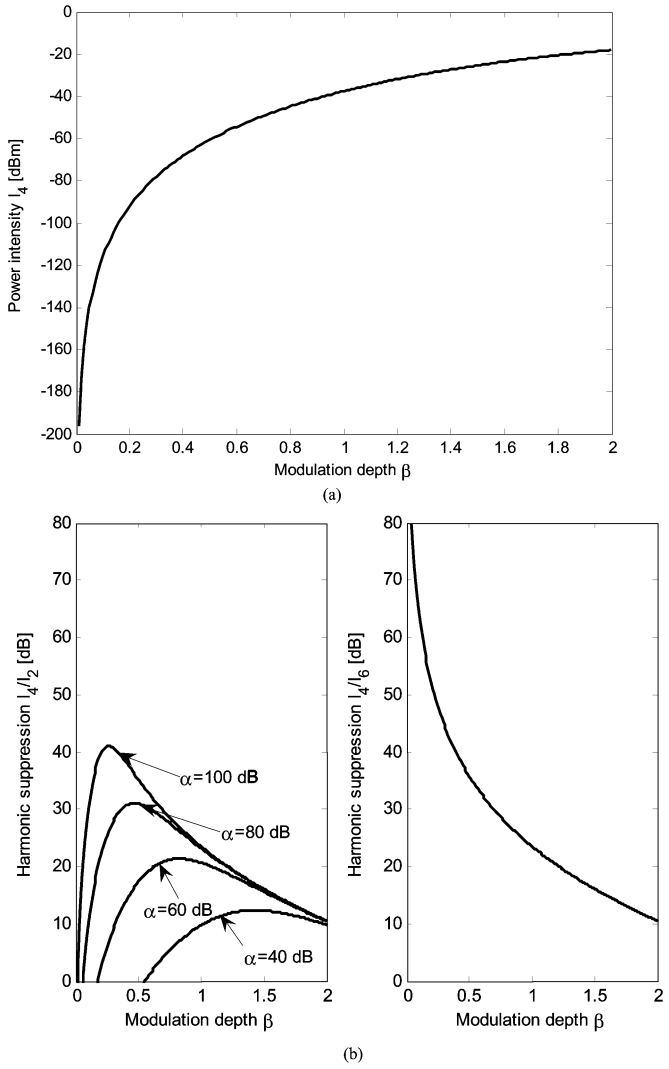

Fig. 4. Power intensity and harmonic suppressions versus modulation depth. (a) Power intensity I_4 of the fourth-order harmonic. (b) Harmonic suppressions I_4/I_2 and I_4/I_6. (Frequency of the electrical drive $f_e = 12.5$ GHz.)

Usually, for a commercially available MZM, the maximum available phase modulation index $\beta_{\max}$ is 2. When $0 \le \beta \le 2$, Bessel functions J_{2n} for $n \ge 1$ are all monotonically increasing with respect to β and monotonically decreasing with respect to the order of Bessel function n, and $J_2(2) = 0.35283$, $J_4(2) = 0.033996$, and $J_6(2) = 0.0012024$. Thus, it is reasonable to ignore the optical sidebands with a Bessel coefficient higher than $J_4(\beta)$ in our discussion. Therefore, (7) can be further simplified to

$$\begin{aligned} E_{\text{out}}(t) \cong\ & E_o k J_0(\beta)\cos(\omega_o t) \\ & - E_o J_2(\beta)\cos(\omega_o t - 2\omega_e t) \\ & - E_o J_2(\beta)\cos(\omega_o t + 2\omega_e t) \\ & + E_o J_4(\beta)\cos(\omega_o t - 4\omega_e t) \\ & + E_o J_4(\beta)\cos(\omega_o t + 4\omega_e t). \end{aligned} \tag{8}$$

Equation (8) shows that the optical signal consists of an attenuated optical carrier and four optical sidebands. The spectrum of this optical signal is illustrated as shown in Fig. 2. The arrow

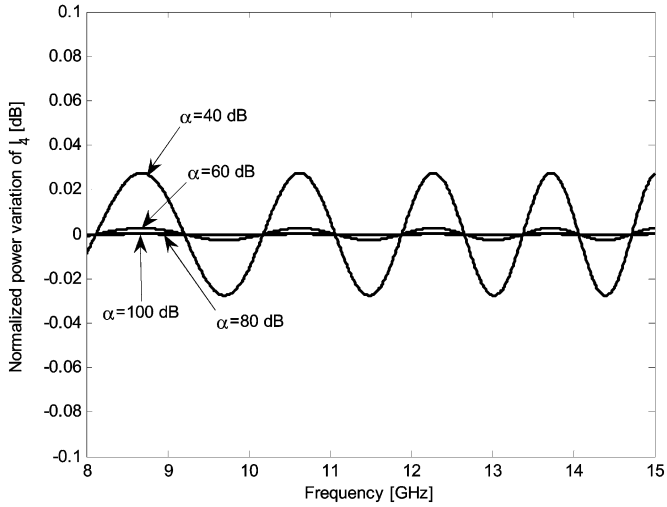

Fig. 5. Power variation of I_4 versus frequency of the electrical drive signal. (Modulation depth $\beta = 0.6$.)

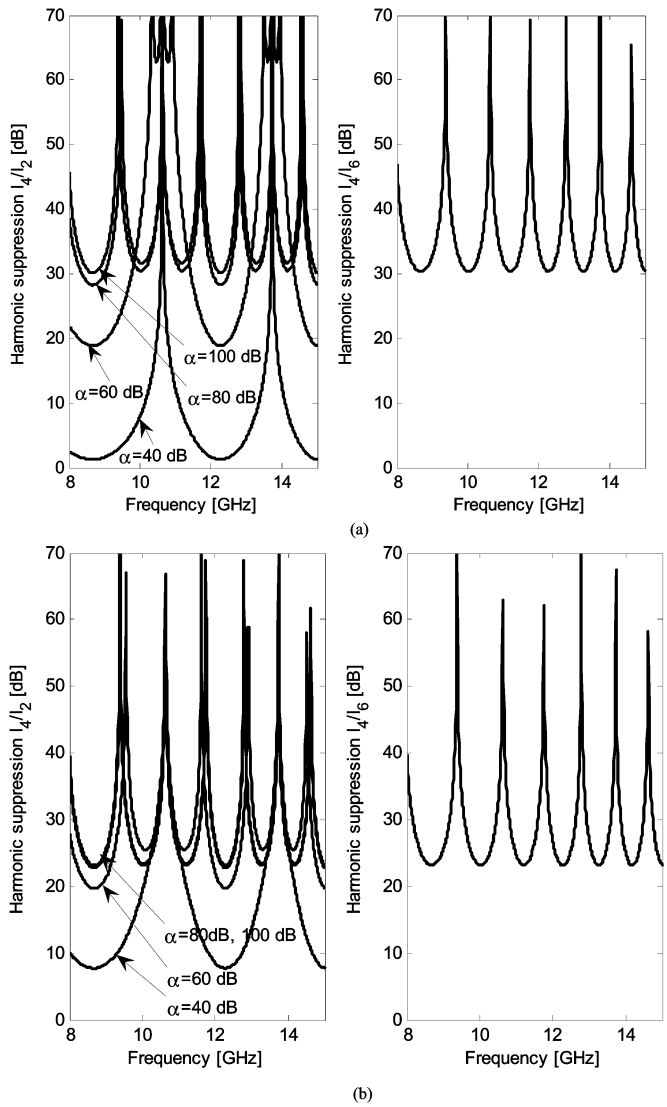

Fig. 6. Harmonic suppressions versus frequency of the electrical drive signal. (a) Modulation depth $\beta = 0.6$. (b) Modulation depth $\beta = 0.9$.

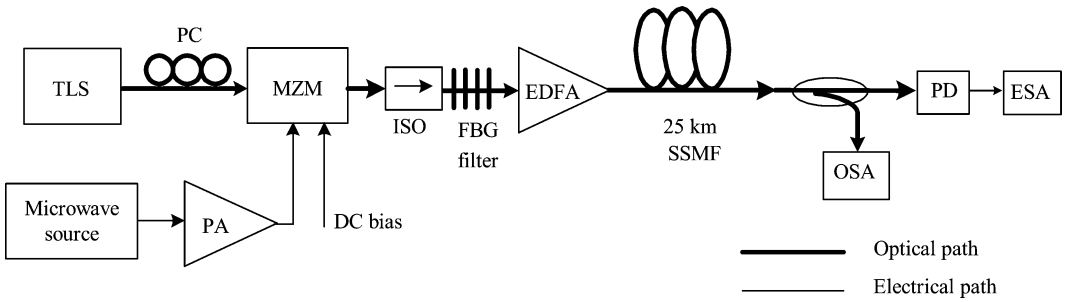

Fig. 7. Experimental setup for optical generation and transmission of millimeter-wave signals. (power amplifier: PA, optical spectrum analyzer: OSA).

direction shows their initial phase with respect to the phase of the optical carrier before transmission.

When the optical signal shown in Fig. 2 is transmitted over a single-mode fiber, the chromatic dispersion of the fiber will cause an extra phase shift to each optical sideband compared to the optical carrier. By expand the propagation constant $\beta(\omega)$ of the fiber for each optical sideband to a Taylor series around the angular frequency of the optical carrier [19], i.e.,

$$\beta(\omega_o \pm 2n\omega_e) = \beta(\omega_o) + \beta'(\omega_o)(\pm 2n\omega_e) + \frac{1}{2}\beta''(\omega_o)(\pm 2n\omega_e)^2 + \cdots \quad (9)$$

where $\beta'(\omega_o)$ and $\beta''(\omega_o)$ are the first- and second-order derivative of the propagation constant $\beta(\omega)$ at the angular frequency ω_o, respectively. The effect of higher order dispersion is neglected for the single-mode fiber at 1550-nm band [20], and $\beta''(\omega_o)$ can be expressed by the chromatic dispersion parameter D as

$$\beta''(\omega_o) = -\frac{c}{2\pi f_o^2} D \quad (10)$$

where c is the speed of light in free space and f_o is the frequency of the optical carrier.

The electric field representing the optical signal at the end of the transmission over a single-mode fiber of length L can be obtained by adding the transmission phase delay $\beta(\omega_0 \pm 2n\omega_e)L$ to the corresponding optical sideband shown in (8). Electrical harmonics will be generated by applying this optical signal to a PD. The output voltage of the generated high-frequency electrical signal is

$$\begin{aligned} V_{\text{out}}(t) \propto & -2E_o^2 \left\{ kJ_0(\beta)J_2(\beta)\cos\left[4\pi cDL\left(\frac{f_e}{f_o}\right)^2\right] \right. \\ & \left. + J_2(\beta)J_4(\beta)\cos\left[12\pi cDL\left(\frac{f_e}{f_o}\right)^2\right] \right\} \\ & \times \cos[2\omega_e t - 2\omega_e \beta'(\omega_o)L] \\ & + E_o^2 \left\{ J_2^2(\beta) + 2kJ_0(\beta)J_4(\beta)\cos\left[16\pi cDL\left(\frac{f_e}{f_o}\right)^2\right] \right\} \\ & \times \cos[4\omega_e t - 4\omega_e \beta'(\omega_o)L] \\ & - 2E_o^2 \left\{ J_2(\beta)J_4(\beta)\cos\left[12\pi cDL\left(\frac{f_e}{f_o}\right)^2\right] \right\} \\ & \times \cos[6\omega_e t - 6\omega_e \beta'(\omega_o)L] \end{aligned} \quad (11)$$

where f_e is the frequency of the electrical drive signal. The electrical spectrum of the generated signal expressed by (11) is illustrated as shown in Fig. 3.

From (11), the power intensity of the fourth-order electrical harmonic I_4 is proportional to the coefficients of optical sidebands

$$I_4 \propto \frac{E_o^4}{2}\left\{ J_2^2(\beta) + 2kJ_0(\beta)J_4(\beta)\cos\left[16\pi cDL\left(\frac{f_e}{f_o}\right)^2\right] \right\}^2. \quad (12)$$

The power intensities of the second- and sixth-order electrical harmonics I_2, I_6 are

$$\begin{aligned} I_2 \propto & 2E_o^4 \left\{ kJ_0(\beta)J_2(\beta)\cos\left[4\pi cDL\left(\frac{f_e}{f_o}\right)^2\right] \right. \\ & \left. + J_2(\beta)J_4(\beta)\cos\left[12\pi cDL\left(\frac{f_e}{f_o}\right)^2\right] \right\}^2 \end{aligned} \quad (13)$$

$$I_6 \propto 2E_o^4 \left\{ J_2(\beta)J_4(\beta)\cos\left[12\pi cDL\left(\frac{f_e}{f_o}\right)^2\right] \right\}^2. \quad (14)$$

For a distribution system that operates at 1550 nm with a transmission distance of 25 km over a standard single-mode fiber with $D = 17$ ps/(nm $\cdot$ km), the power intensity I_4 and harmonic suppressions of I_4/I_2 and I_4/I_6 versus the modulation depth β ($0 \le \beta \le 2$) are plotted in Fig. 4.

Fig. 4(a) shows that the power intensity I_4 is monotonically increasing for $0 \le \beta \le 2$, and Fig. 4(b) shows that the harmonic suppression I_4/I_2 is monotonically decreasing for $0.5 \le \beta \le 2$ and $\alpha \ge 80$ dB, and for $0.25 \le \beta \le 2$ and $\alpha \ge 100$ dB; the harmonic suppression I_4/I_6 is monotonically decreasing for $0 \le \beta \le 2$, which is independent of the attenuation α of the optical notch filter. With a large attenuation of the optical notch filter, a lower modulation depth corresponds to an improved harmonic suppression. As can be seen from Fig. 4(b), for $\alpha = 100$ and $0.25 \le \beta \le 2$, the lower the modulation depth, the higher the harmonic suppression. However, lower modulation depth leads to a lower output power of the fourth-order electrical harmonic, as shown in Fig. 4(a). This problem can be solved at a low cost by using erbium-doped fiber amplifiers (EDFAs) in the 1550-nm band. Note that a lower modulation depth means a less power requirement for the electrical drive signal.

Fig. 5 shows the power variation of the generated electrical signal I_4, which is caused by the combined effects of the limited attenuation of the optical carrier and the chromatic dispersion of the fiber when tuning the frequency of the electrical drive signal

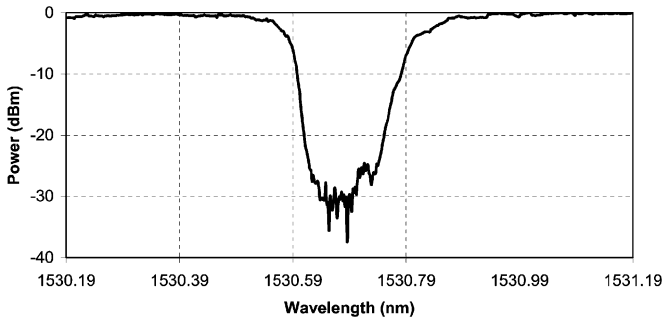

Fig. 8. Transmission spectrum of the FBG filter.

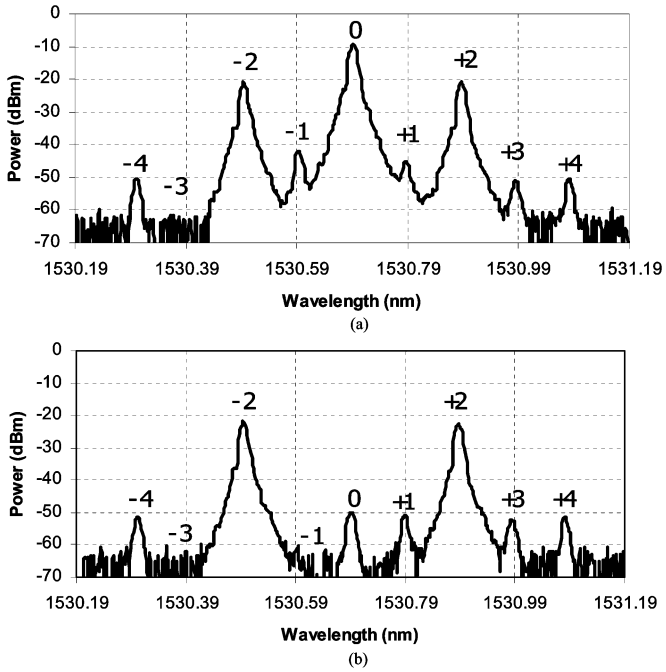

Fig. 9. Optical spectra before transmission. (a) Before the FBG filter. (b) After the FBG filter.

from 8 to 15 GHz. It is clearly seen that when $\alpha \geq 40$ dB, this power variation is smaller than 0.03 dB. That means the amplitude of the frequency-quadrupled electrical signal is stable over the tuning band when β is a constant and $\alpha \geq 40$ dB. Small ripples found in Fig. 5 are caused by the chromatic dispersion of the 25-km single-mode fiber. Fig. 6(a) shows that when the modulation depth $\beta = 0.6$, the minimum value of I_4/I_2 is around 2 dB with $\alpha = 40$ dB, greater than 18.5 dB with $\alpha = 60$ dB, 28.3 dB with $\alpha = 80$ dB and 30 dB with $\alpha = 100$ dB; the minimum value of I_4/I_6 is greater than 30 dB and is independent of α. That means, with a small value of modulation depth, the harmonic suppression is mostly affected by the attenuation of the optical notch filter. Fig. 6(b) indicates that with a small value of the attenuation of the optical notch filter, increasing the modulation depth of the MZM from 0.6 to 0.9 improves the harmonic suppression. The minimum value of I_4/I_2 has increased from 2 to 7.7 dB for $\alpha = 40$ dB case, and 18.5 to 19.7 dB for $\alpha = 60$ dB case.

III. Experiment

In order to validate the proposed method and verify the analysis, the experimental setup shown in Fig. 7 is built. The quality of the generated millimeter-wave signal is evaluated both before (local signal) and after (remote signal) propagation over 25 km of SSMF. Light from a tunable laser source (TLS) is applied to

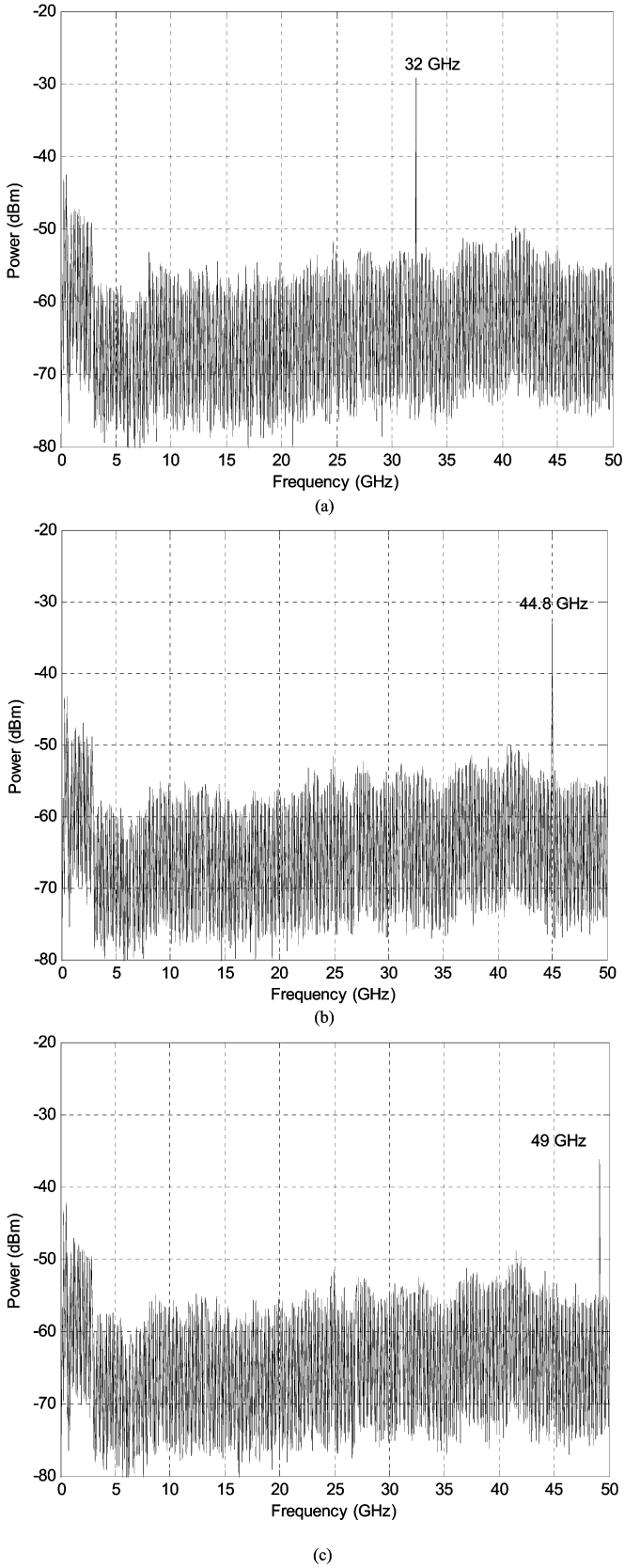

Fig. 10. Spectra of the generated millimeter-wave signals. (a) 32 GHz. (b) 44.8 GHz. (c) 49 GHz.

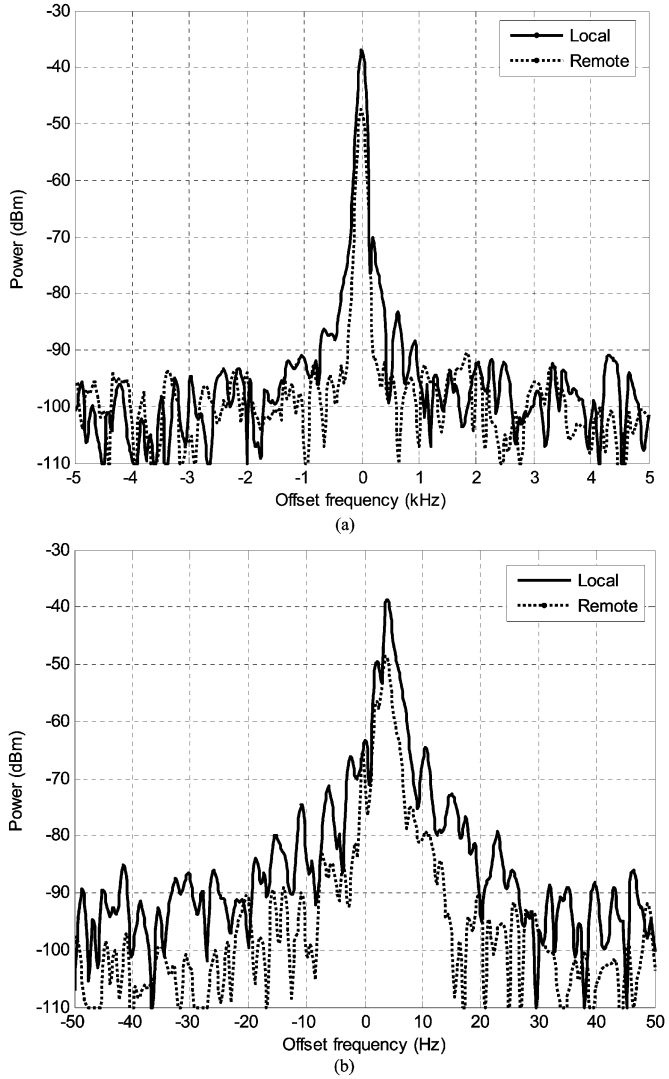

Fig. 11. Spectra of the 50-GHz signal generated locally and remotely. (a) Frequency span: 10 kHz. (b) Frequency span: 100 Hz.

the MZM via a polarization controller (PC). The MZM is a commercially available lithium–niobate modulator, which is biased to suppress all the odd-order optical sidebands. An FBG filter with a central wavelength equal to the wavelength of the optical carrier is used as an optical notch filter. The optical carrier is removed at the output of the FBG filter. The transmission spectrum of the FBG filter is shown in Fig. 8. The bandwidth from the minimum attenuation point at lower wavelengths to the minimum attenuation point at longer wavelengths is approximately 0.3 nm ($\approx$ 37.5 GHz).

A 25-dBm microwave signal with frequencies tunable from 8 to 15 GHz is used to drive the MZM. By appropriately adjusting the dc-bias voltage of the MZM, the odd-order optical sidebands are suppressed, as indicated by (3). The optical spectrum at the output of the MZM is shown in Fig. 9(a). The optical carrier is then suppressed by the FBG filter. The optical spectrum is shown in Fig. 9(b).

Fig. 10 shows the spectra of the generated electrical signals when the microwave drive signal is tuned at 8, 11.2, and 12.25 GHz. Beat signals with frequencies four times that of the drive signals are generated. It can be seen from Fig. 10 that millimeter-wave signals at the frequency of 32, 44.8, and 49 GHz are generated. The spectra are very clean, no other beat signals can be observed across the 50-GHz band.

Fig. 11 gives zoom-in views of the beating signal generated locally and remotely after transmission over a 25-km signal-mode fiber. The frequency of the electrical drive signal is tuned at 12.5 GHz, the generated millimeter-wave signal is at 50 GHz. As can be seen, the signal quality of the remotely generated signal is maintained, which demonstrates that the signal is not seriously affected by the chromatic dispersion of the 25-km single-mode fiber.

The lowest frequency (32 GHz) that can be generated by the proposed system is determined by the bandwidth of the FBG notch filter. With a narrower optical notch filter, this frequency could be much lower than 32 GHz. On the other hand, the highest frequency of the generated signal is only limited by the bandwidth of the optical intensity modulator. The intensity modulator used in the experiment can operate up to 15 GHz so the highest frequency of the generated millimeter-wave signal can reach up to 60 GHz. Due to the bandwidth limitation of the PD and the electrical spectrum analyzer, the 60-GHz signal was not observed in the electrical domain. However, optical spectrum observation supports the 60-GHz signal generation.

IV. Conclusion

We have proposed and demonstrated a novel microwave-photonics system that could generate and distribute a broadband frequency-tunable millimeter-wave signal using a low-frequency intensity modulator and a wavelength-fixed optical notch filter. The technique was based on the nonlinear response of the intensity modulator by properly biasing it to suppress the odd-order optical sidebands. The optical carrier was then removed by the optical notch filter. Since no tunable optical filter was used, the system was easy to implement. Theoretical analysis on the harmonic suppression with different modulation depths and filter attenuations was discussed. A system using an $LiNbO_3$ intensity modulator and an FBG filter was built. The results have shown that a stable high spectral-purity millimeter-wave signal from 32 to 50 GHz was directly observed on an electrical spectrum analyzer by tuning an electrical drive signal from 8 to 12.5 GHz. The generated millimeter-wave signal was distributed over 25-km standard single-mode fiber; the integrity of the generated millimeter-wave signal at the end of the fiber span was maintained after the transmission.

Acknowledgment

The authors would like to thank J. Oldham, Communications Research Centre, Ottawa, ON, Canada, D. Barlow, Communications Research Centre, F. Zeng, School of Information Technology and Engineering, University of Ottawa, Ottawa, ON, Canada, and X. Chen, School of Information Technology and Engineering, University of Ottawa, for their assistance in setting up the experimental system.

References

[1] A. J. Cooper, "Fiber/radio for the provision of cordless/mobile telephony services in the access network," *Electron. Lett.*, vol. 26, no. 24, pp. 2054–2056, 1990.

[2] A. J. Seeds, "Broadband wireless access using millimeter-wave over fiber systems," in *IEEE MTT-S Int. Microwave Symp.*, 1997, Paper TU1B-1, pp. 23–25.
[3] R. P. Braun, G. Grosskopf, D. Rohde, and F. Schmidt, "Optical millimeter-wave generation and transmission experiments for mobile 60 GHz band communications," *Electron. Lett.*, vol. 32, no. 7, pp. 626–628, 1996.
[4] H. Ogawa, D. Polifko, and S. Bamba, "Millimeter-wave fiber optics systems for personal radio communications," *IEEE Trans. Microw. Theory Tech.*, vol. 40, no. 12, pp. 2285–2293, Dec. 1992.
[5] L. Nöel, D. Wake, D. G. Moodie, D. D. Marcenac, L. D. Westbrook, and D. Nesset, "Novel techniques for high capacity 60 GHz fiber-radio transmission systems," *IEEE Trans. Microw. Theory Tech.*, vol. 45, no. 8, pp. 1146–1423, Aug. 1997.
[6] H. Schmuck, "Comparison of optical millimeter-wave system concepts with regard to chromatic dispersion," *Electron. Lett.*, vol. 31, no. 21, pp. 1848–1849, 1995.
[7] U. Gliese, S. Nørskov, and T. N. Nielsen, "Chromatic dispersion in fiber-optic microwave and millimeter-wave links," *IEEE Trans. Microw. Theory Tech.*, vol. 44, no. 10, pp. 1716–1724, Oct. 1996.
[8] G. H. Smith, D. Novak, and Z. Ahmed, "Overcoming chromatic-dispersion effects in fiber-wireless systems incorporating external modulators," *IEEE Trans. Microw. Theory Tech.*, vol. 45, no. 8, pp. 1410–1415, Aug. 1997.
[9] R. Hofstetter, H. Schmuck, and R. Heidemann, "Dispersion effects in optical millimeter-wave systems using self-heterodyne method for transport and generation," *IEEE Trans. Microw. Theory Tech.*, vol. 43, no. 9, pp. 2263–2269, Sep. 1995.
[10] L. Goldberg, H. F. Taylor, J. F. Weller, and D. M. Bloom, "Microwave signal generation with injection-locked laser diodes," *Electron. Lett.*, vol. 19, no. 13, pp. 491–493, 1983.
[11] T. Jung, J.-L. Shen, D. T. K. Tong, S. Murthy, M. C. Wu, T. Tanbun-Ek, W. Wang, R. Lodenkamper, R. Davis, L. J. Lembo, and J. C. Brock, "CW injection locking of a mode-locked semiconductor laser as a local oscillator comb for channelizing broad-band RF signals," *IEEE Trans. Microw. Theory Tech.*, vol. 47, no. 7, pp. 1225–1232, Jul. 1999.
[12] T. Ramos and A. J. Seeds, "Fast heterodyne optical phase lock loop using double quantum well laser diodes," *Electron. Lett.*, vol. 28, no. 1, pp. 82–83, 1992.
[13] M. Hyodo, K. S. Abedin, and N. Onodera, "High-purity, optoelectronic millimeter-wave signal generation by heterodyne optical phase-locking of external-cavity semiconductor lasers," presented at the Lasers Electro-Optics Eur., Sep. 10–15, 2000, Paper CTuP2.
[14] F. N. Timofeev, S. Bennett, R. Griffin, P. BayveL, A. J. Seeds, R. Wyatt, R. Kashyap, and M. Robertson, "High spectral purity millimeter-wave modulated optical signal generation using fiber grating lasers," *Electron. Lett.*, vol. 34, no. 7, pp. 668–669, Apr. 1998.
[15] J. J. O'Reilly, P. M. Lane, R. Heidemann, and R. Hofstetter, "Optical generation of very narrow linewidth millimeter wave signals," *Electron. Lett.*, vol. 28, no. 25, pp. 2309–2311, 1992.
[16] J. J. O'Reilly and P. M. Lane, "Remote delivery of video services using mm-wave and optics," *J. Lightw. Technol.*, vol. 12, no. 2, pp. 369–375, Feb. 1994.
[17] ——, "Fiber-supported optical generation and delivery of 60 GHz signals," *Electron. Lett.*, vol. 30, no. 16, pp. 1329–1330, 1994.
[18] P. Shen, N. J. Gomes, P. A. Davies, W. P. Shillue, P. G. Huggard, and B. N. Ellison, "High-purity millimeter-wave photonic local oscillator generation and delivery," in *Proc. Int. Microwave Photonics Topical Meeting*, Sep. 10–12, 2003, pp. 189–192.
[19] K. Okamoto, *Fundamentals of Optical Waveguides*. New York: Academic, 2000, pp. 72–72.
[20] W. K. Marshall, B. Crosignani, and A. Yariv, "Laser phase noise to intensity noise conversion by lowest-order group-velocity dispersion in optical fiber: Exact theory," *Opt. Lett.*, vol. 25, no. 3, pp. 165–167, 2000.

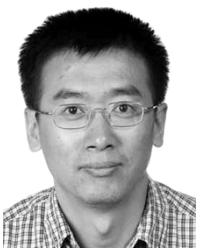

Guohua Qi received the B.E. and M.S. degrees in electrical engineering from the Beijing University of Posts and Telecommunications, Beijing, China, in 1986 and 1989, respectively, and is currently working toward the Ph.D. degree in information technology and engineering at the University of Ottawa, Ottawa, ON, Canada.

In 1989, he joined the Nanjing Electronic Devices Institute (NEDI), Nanjing, China, where he was engaged in the research and development of microwave solid-state circuits, modules, and subsystems for the next 12 years. His current research interests include microwave photonics, radio over fiber, and SDR.

Jianping Yao (M'99–SM'01) received the Ph.D. degree in electrical engineering from the University of Toulon, France, in 1997.

He is currently an Associate Professor with the School of Information Technology and Engineering, University of Ottawa, Ottawa, ON, Canada. From January 1998 to July 1999 he was a Research Fellow, and from July 1999 to December 2001, he was an Assistant Professor, both with the School of Electrical and Electronic Engineering, Nanyang Technological University, Singapore. From January to March 2005, he was an Invited Professor with the Institut National Polytechnique de Grenoble, Grenoble, France. He has authored or coauthored over 100 papers in refereed journals and conference proceedings. His current research interests include optical signal processing, optically controlled phased-array antennas, photonic generation of microwave signals, radio-over-fiber systems, fiber lasers and amplifiers, broad-band infrared wireless home networking, and fiber-optic sensors.

Dr. Yao is a member of The International Society for Optical Engineers (SPIE) and the Optical Society of America (OSA).

Joe Seregelyi received the M.Eng. degree in engineering physics from McMaster University, Hamilton, ON, Canada, in 1987.

In 1988, he joined the National Research Council, where he was involved in the area of pulsed electromagnetics. Since 1993, he has been with the Communications Research Centre, Ottawa, ON, Canada, where he is currently the Research Engineering/Project Leader of microwave photonics. He has authored or coauthored over 50 technical papers and reports. He holds patents in the area of hybrid infrared (IR)/high-power microwaves (HPM) landmine detection and neutralization. He possesses extensive knowledge in the areas of RF and microwave design (signal integrity, circuit design, electromagnetic compatibility, antenna design, HPMs, and ultra-wideband radar and communications). He has also been involved with optical design for a number of years (high-power lasers, antenna remoting, communications systems and IR imaging).

Stéphane Paquet received the M.Sc. degree in optics from Laval University, Quebec, QC, Canada, in 1993.

He then joined the National Optics Institute, where he was involved with the design and fabrication of integrated optics components. He then joined MPB Technologies, Montreal, QC, Canada, as a member of the Space Technology Group and Optical Amplifier Research and Development Group. In 1997, he joined Nortel Networks, Montreal, QC, Canada, where he was initially a member of the Communication Systems Engineering Group. He was then an Optical System Designer with Nortel Networks, Ottawa, ON, Canada, and a Researcher with the Optical Components Research and Development Group, Nortel Networks, Harlow, U.K. He is currently with the Communications Research Centre, Ottawa, ON, Canada, where he is involved in the microwave photonic research field.

Claude Bélisle received the Bachelor's degree in engineering physics from the Royal Military College of Canada, Kingston, ON, Canada, and the Master's degree in physics-optics from Laval University, Quebec, QC, Canada.

He has been involved in various research and development projects related to satellite communications for both military and commercial applications with the DRDC–Ottawa and Communications Research Centre, Ottawa, ON, Canada. He is currently the Research Manager of the CRC Advanced Radio System Group, where he leads research in microwave-photonics technologies, satellite communications networks, and SDR. He is also a Director of the Software Defined Radio Forum.